



## Fracture resistance of cracked duplex stainless steel elbows under bending with or without internal pressure

Sémété P., Le Delliou P., Ignaccolo S.  
EDF, France

**ABSTRACT :** EDF, in co-operation with Framatome, has conducted a research programme on the fracture resistance of thermally aged cast duplex stainless steel elbows. The main task of this programme consisted in testing three 2/3-scale models of PWR primary loop cast elbows. The first two tests (SEM1 and SEM2) were conducted under in-plane closure bending at 320°C and the third one (SEM3) under constant internal pressure and in-plane closure bending at 60°C. This paper presents the experimental results, some numerical results and finally the ductile fracture mechanics analyses.

### 1 INTRODUCTION

EDF, in co-operation with FRAMATOME, has conducted a research programme on the fracture behaviour of aged cast duplex stainless steel elbows [1]. The main task of this programme consisted in testing three large diameter elbows under in-plane closure bending with or without internal pressure.

The first two tests (under in-plane closure bending only, at 320°C) were already presented in a previous paper [2]. The corresponding results are summarised hereafter and are complemented by the results obtained with the third test for which the elbow was loaded with internal pressure and in-plane bending at 60°C. This paper presents the experimental results, the numerical computations and the fracture mechanics analyses that were performed for the three tests.

### 2 TEST DESCRIPTION

#### 2.1 Description of the elbows

The elbows were made of Z3 CND 19-10M duplex stainless steel (French standard equivalent to CF8M). Prior to the tests, the first two elbows were thermally aged during 3,000 hours at 400°C and the third one was aged 1,000 hours at 400°C. Their dimensions are the following :

- outer diameter : 580 mm
- thickness : 44 mm
- bend radius : 900 mm
- bend angle : 90 degrees.

The elbows of the first two tests contained a semi-elliptical machined notch on the outer surface of one flank and were loaded under in-plane closure bending. For each elbow, the crack was located so that it was submitted to tensile stresses. The characteristics of the notches are represented on Figure 1.

For the third test, the elbow contained both cracks previously described (one on each flank) and was loaded with a constant internal water pressure of 15.5 MPa and under in-plane closure bending.

### 2.2 Description of the test conditions

The test facility used by Electricité de France (EDF) is called « SEM » and is schematically represented in Figure 2. The moment loading is generated by pulling on the arm pipe with a long stroke ram.

For the third test, where, in addition to the moment loading, an internal pressure of water at 15.5 MPa was applied, two flat heads were inserted : one between the elbow and the flange and the other one between the connecting pipe and the arm pipe.

During the first two tests, the elbow and the connecting pipes were heated at 320°C, while for the third test, the elbow, the flat heads, and the connecting pipe were maintained at 60°C.

### 2.3 Material data

The material characterisation programme included chemical analysis, tensile tests and J-resistance curves determined on 1T-CT specimens. For the duplex stainless steel elbows, the chemical composition (especially elements contents like Cr, Mo, Ni and  $\delta$  ferrite) leads to a severe thermal aging and low toughness values after thermal aging at 400°C.

For the elbows, the connecting pipes and the flat heads which behave plastically, conventional tensile properties are given in Table 1 and true stress - true strain curves are shown in Figure 3. For the other components (flange, loading saddle and arm pipe) which remained elastic during the tests, we give their Young modulus in Table 1.

TABLE 1 - Mechanical properties of the three test materials

Material I.D.	Test temperature (°C)	Young's modulus (MPa)	0.2% offset yield strength (MPa)	Ultimate tensile strength (MPa)
SEM1/cast elbow	320	176500	258	670
SEM2/cast elbow	320	175500	259.5	662
SEM3/cast elbow	60	188000	321	743
Connecting pipes/SEM1 & 2	320	188000	223	545
Connecting pipes/SEM3	60	201000	278.4	-
Flat heads/SEM3	60	201000	460	-
Arm pipe/SEM1 & 2 & 3	20	204000	-	-
Flange/SEM1 & 2	320	183000	-	-
Flange/SEM3	60	201000	-	-
Loading saddle/SEM1 & 2 & 3	20	204000	-	-

The connecting pipes, the flat heads, the arm pipe, the flange, and the loading saddle were made with carbon steel.

Toughness tests (at 320°C for SEM1 & 2 and 60°C for SEM3) carried out on aged duplex steel CT25 (1T-CT) specimens have given the values of  $J_{0.2}$  (value of J for 0.2 mm of crack extension) and a J-R curve fitted by a power-law,  $J = C(\Delta a)^n$ . The J-R curves exhibit some scatter and a statistical analysis of the data was used to give the results provided in Table 2.

TABLE 2 - Toughness properties of the three elbows

Material I.D.	Test temperature (°C)	$J_{0.2}$ mean value (kJ/m <sup>2</sup> )	C mean value (kJ/m <sup>2</sup> )	n mean value ( $\Delta a$ in mm)
SEM1 cast elbow	320	68	97.2	0.2497
SEM2 cast elbow	320	51	66.6	0.1796
SEM3 cast elbow	60	56	84.13	0.2698

#### 2.4 Test results

For the first two tests, the bending load was applied at a quasi-static rate, with a ram displacement rate of 2 mm/min. For the third test, the pressurisation of the elbow was realised first, then the bending moment was applied in the same way as described before.

During the tests, several measurements were made : applied load, ram displacement, elbow diameter variations (for ovalization), structure rotation (with inclinometers), CMOD in several points along the crack length, and strains in the elbow mid plane. Direct-current electric potential drop method was used to detect crack initiation and to conduct the tests (i.e. to obtain a given amount of stable crack extension).

For each test, the crack (see figure 1) was located in a tensile stresses area, so that it initiated and grew subsequently by ductile tearing. The final crack extension reached 8 mm (first test) and 13 mm (second test). The third elbow, tested with internal pressure, contained both cracks described previously (one on each flank). The longitudinal one initiated first and its final extension reached more than 6 mm while, for the circumferential one, the final extension was only 2.6 mm long.

Applied load versus ram displacement curves are shown for the three tests in Figure 4. First two tests curves are very close together, due to the similarity of the stress-strain curves (see Figure 3). This proves that the influence of the crack is relatively small on the global load versus displacement curve. The third test curve is stiffer than the other, because the internal pressure and the flat heads limited the ovalization of the elbow and, also, the stress-strain curve of its material at lower temperature (60°C instead of 320°C) was stiffer.

Table 3 summarises the main results of the three tests ( $F_y$  is the applied load on the loading point normal to the moment arm and the moment is evaluated in the mid section of the elbow taking into account the moment due to the dead weight of the structure).

TABLE 3 - Main results of the tests

Test I.D.	Crack initiation Fy (kN)	End of test Fy (kN)	End of test moment (kN.m)	End of test $\Delta a$ (mm)
SEM1	363 / 378	464	2705	8
SEM2	194 / 215	483	2900	12
SEM3	365 / 391 (longi. notch)	531	3150	6.3 (longi. notch)
	405 / 426 (circum. notch)			2.6 (circum. notch)

As explained in [2], the final crack shape was optically measured and, because of its irregular shape, was smoothed by a semi-ellipse for the purpose of the analyses.

### 3 NUMERICAL ANALYSIS

#### 3.1 Description of the FE models

The calculations were made with the FE code named *Code\_Aster*® developed by EDF. The meshes of the test structures were built up with solid elements (15 and 20 node elements) and, in addition for the third test, with shell elements (6 and 8 node elements) in order to apply internal pressure.

The mesh is elaborated from a cracked block (see Figure 5) which is characterised by a refinement relevant to fracture mechanics analyses. Due to the small size of the notch, it was assumed that its presence had no influence on the global behaviour of the structure (i.e. in terms of load versus displacement curve). This was verified by an elastic-plastic computation of the uncracked structure and by the test results as described in the previous paragraph. This enabled to model half structure with a notch (it means that the corresponding full model has, in fact, two symmetrical cracks). The third elbow mesh included the flat heads as shown at the top of the Figure 5. The main characteristics of the meshes are indicated in Table 4.

TABLE 4 - Size of FE models

Test I.D.	Nodes	Solid elements	Shell elements
SEM1	12014	2746	-
SEM2	12142	2778	-
SEM3 (longi. notch)	16103	3670	1260
SEM3 (circum notch)	14259	3228	1280

#### 3.2 Global behaviour of the tested structure

The simulation results about the global behaviour of the structure were expressed in terms of load versus ram displacement curves (where Fy is the applied load on the loading point normal to the moment arm and Uy is the displacement of this same point also normal to the moment arm). These curves are given in Figure 4.

The first two test computations were made with a large displacement formulation which takes into account the effect of softening due to the elbow ovalization. Moreover, we simulated the dead weight whose effect is not negligible ( $\approx 160 \text{ kN.m}$ ).

Finally, for the third test, the application of internal pressure on the updated geometry within the framework of the large displacement formulation provides another improvement for the global behaviour simulation. However, in this case, the internal pressure and the flat heads limited the elbow ovalization so that the small displacement formulation gave also very good results.

### 3.3 Crack initiation evaluation

The crack initiation evaluation used the 3-D energy release rate (parameter  $G$ ) calculated in the center of the crack. The  $G$  parameter versus applied load  $F_y$  curve is then compared with the toughness  $J_{0.2}$  obtained with 1T-CT specimens in order to predict the load at crack initiation.

The energy release rate is calculated using the G-THETA method developed by EDF [3, 4]. A new formulation for the energy release rate parameter  $G$  was developed to be consistent with the « large displacement » option [5] and was used for the first two test computations. According to the observation made at the end of the previous section for the third test, the  $G$  computations were made with the small displacement formulation.

For the three tests, the crack initiation is correctly predicted or in slightly conservative manner using the mean value of the parameter  $J_{0.2}$ . Those results are presented in Figure 6 for the longitudinal and the circumferential cracks of SEM3 test (those for SEM1 and SEM2 were presented in [2]). We can notice on Figure 6 that, until the initiation load is reached, the  $G$  value is higher for the longitudinal crack than for the circumferential one. This is quite consistent with the test results where the longitudinal crack effectively initiated first. Rigorously, this calculation with the initial crack mesh is no longer valid once the crack begins to propagate. In the following paragraph, we will verify that the computations with deeper cracks (accounting for crack growth) still respect the fact that the longitudinal crack grew faster than the circumferential one during this third test.

### 3.4 Crack growth evaluation

This evaluation is made on a  $J$ - $\Delta a$  diagram by comparing the applied- $J$  curves (obtained from the calculations) with the material  $J$ - $R$  curve (obtained on CT specimens). The applied- $J$  curves are obtained for different levels of loading from calculations of the parameter  $G$  made with meshes containing cracks of different depths.

Except for the SEM3 circumferential crack analysis, the material  $J$ - $R$  curves were extrapolated beyond 3 mm (which is the validity limit for CT25 specimens) with the power-law fit determined in the validity range. For each material, a mean curve, a minimum one ( $-2\sigma$ ) and a maximum one ( $+2\sigma$ ) were assessed.

As detailed in a previous paper [2], the numerical prediction was conservative for SEM1 test and very conservative for SEM2 test, which exhibited some geometrical or constraint effect. The results of SEM3 crack growth evaluation are shown in Figure 7 for the longitudinal notch and in Figure 8 for the circumferential one.

For the longitudinal notch of the SEM3 test, the prediction is conservative with the mean curve. For the circumferential notch of the SEM3 test, the prediction is also conservative with the mean curve (i.e. the final propagation of 2.6 mm is obtained for a calculated load  $F_y$  lower

than the experimental one). Also, as it was presented in the previous part, we effectively observe, comparing the increase of  $G$  for different crack depths versus applied load in Figures 7 and 8, that the simulations are consistent with the fact the longitudinal crack grew faster than the circumferential one during the test.

#### 4 CONCLUSIONS

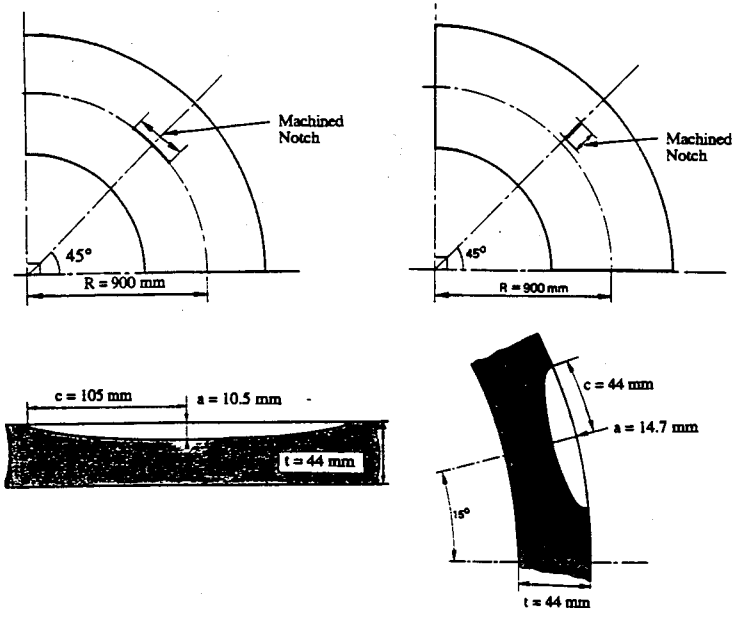
EDF performed three bending tests, with or without internal pressure, on large diameter aged cast duplex stainless steel elbows containing one or two semi-elliptical notches on the flank. The first two elbows, loaded under in-plane closure bending, each contained one semi-elliptical notch on the outer surface of flank. The third elbow, loaded under in-plane closure bending and internal pressure of 15.5 MPa, contained both previous semi-elliptical notches, one on each flank.

The tests showed that it was possible to obtain a large amount of stable crack growth despite the low toughness properties of the thermally aged material. Thanks to the good efficiency of the direct-current electric potential method, the crack initiation was accurately detected and the final crack extension was correctly predicted.

The finite element analyse of the three tests, were in very good agreement with the global behaviour of each structure test and enabled us to give a good prediction of the crack initiation in each case. The crack growth analysis is conservative. Three reasons are proposed to explain this fact : the scatter of the J-R data, the extrapolation of J-R curves to longer crack extension and a constraint effect in the ligament.

#### REFERENCES

1. Eripret Ch., Le Delliou P. & Masson J.C. 1990. Study of cast duplex stainless steel elbow under closure bending  
*Proceedings ECF8*: Vol. 3, pp 1570-1575.
2. Le Delliou P., Sémété P. & Ignaccolo S. 1996. Fracture mechanics analysis of cast duplex stainless steel elbows containing a surface crack  
*Proceedings PVP Division Conference*: Vol 323, pp 117-123.
3. Xiao-Zheng Suo & Combescure A. 1992. On the application of  $G(\Theta)$  method and its comparison with De Lorenzi's approach  
*Proceedings Nuclear Engineering and Design*: Vol. 135, pp 207-224.
4. Wadier Y. & Malak O. 1989. The THETA method applied to the analysis of 3-D elastic-plastic cracked bodies  
*Proceedings SMIRT 10*: Vol. G, pp 13-18. Anaheim.
5. Mialon P. & Visse E. 1995. An energy release rate formulation for large deformation problems (in French)  
*Proceedings 2ème Colloque National en Calcul des Structures*: Vol. 1, pp 89-94. Giens.



**SEM1 and SEM3 TESTS**  
 semi-ellipse :  $c/a = 10$   $a/t = 1/4$

**SEM2 and SEM3 TESTS**  
 semi-ellipse :  $c/a = 3$   $a/t = 1/3$

**FIGURE 1 - Notch location and shape**

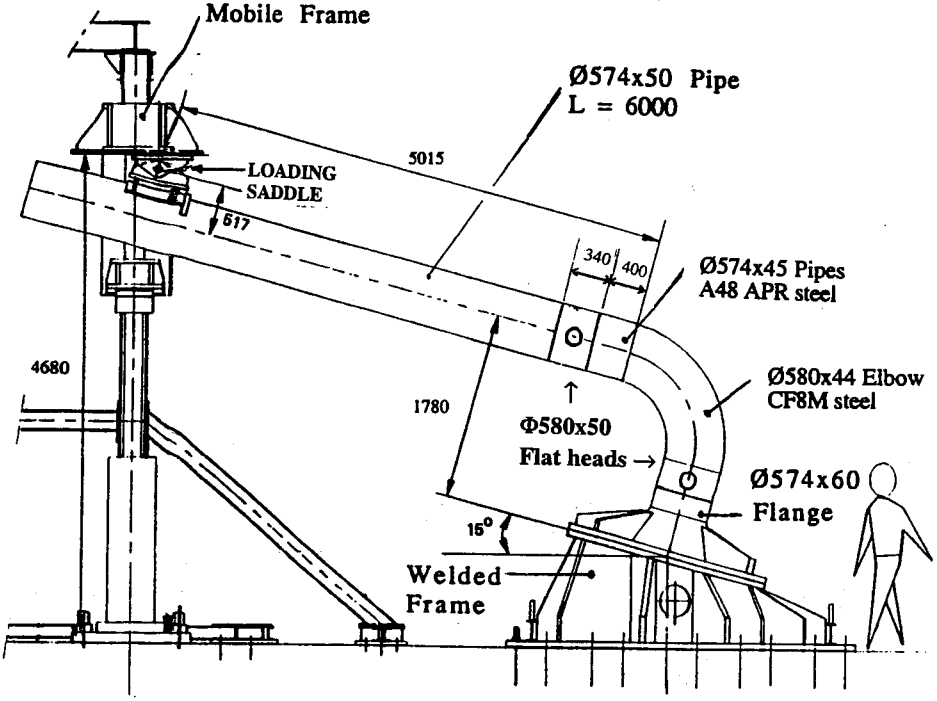


**FIGURE 2 - Schematic drawing of the test facility (third test configuration)**

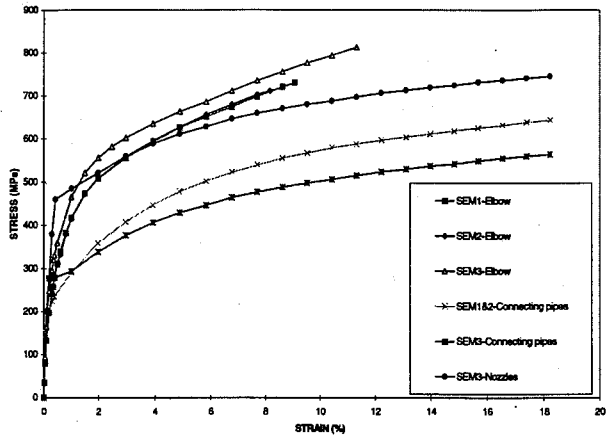


FIGURE 3 - True stress - true strain curves for SEM1, SEM2 and SEM3 tests

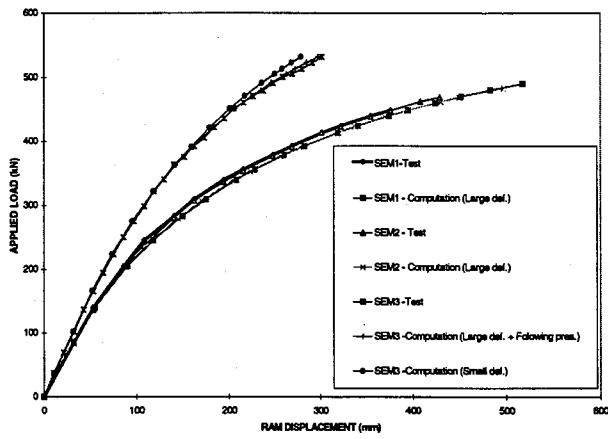


FIGURE 4 - Applied load versus ram displacement

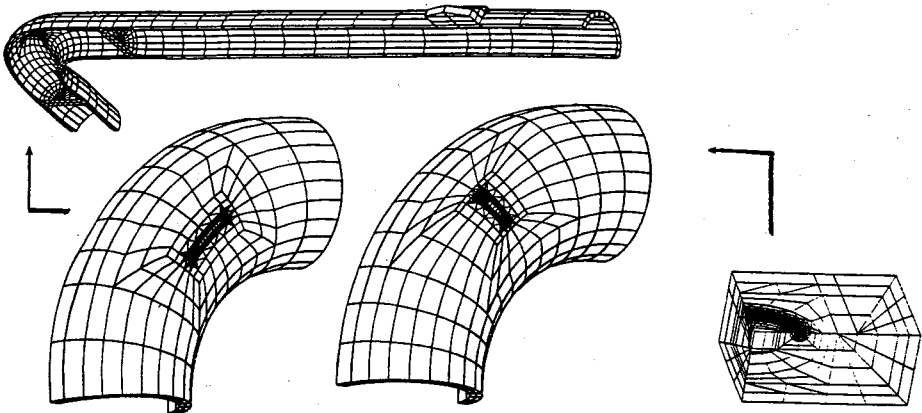


FIGURE 5 - View of the final element mesh (SEM3 test)

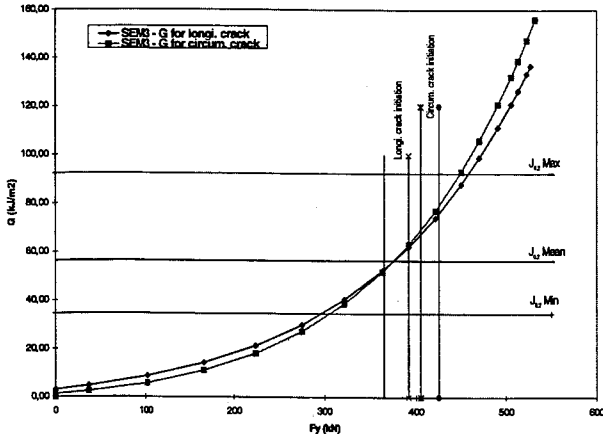


FIGURE 6 - G versus applied load curves (SEM3 test).

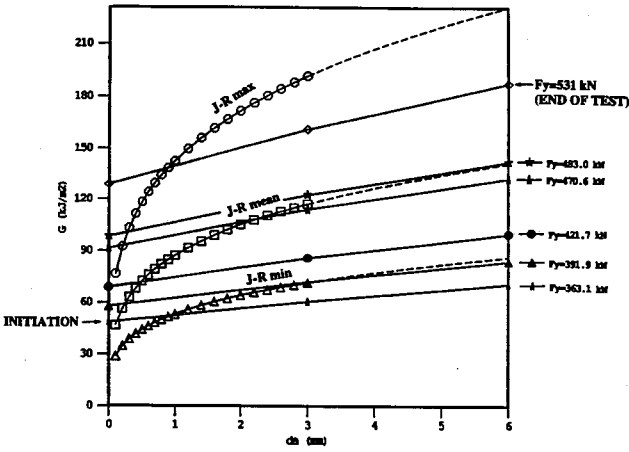


FIGURE 7 - Crack growth analysis for the longitudinal crack of SEM3

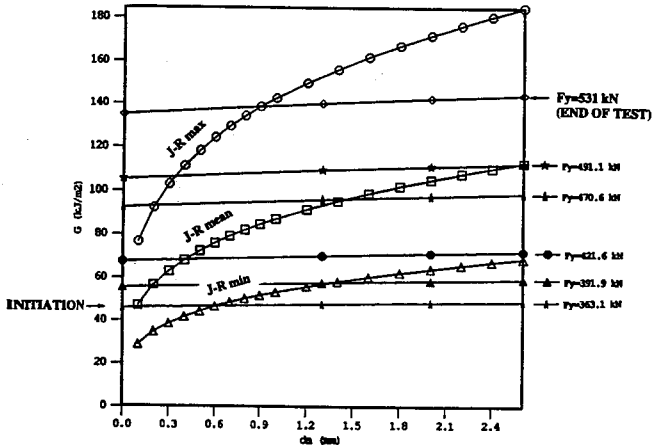


FIGURE 8 - Crack growth analysis for the circumferential crack of SEM3

